Geomechanics and Engineering, *Vol. 11, No. 2 (2016) 269-288*
DOI: http://dx.doi.org/10.12989/gae.2016.11.2.269

Analysis of stress distribution around tunnels by hybridized FSM and DDM considering the influences of joints parameters

Nooraddin Nikadat* and Mohammad Fatehi Marji [a]

Department of Mine Exploitation Engineering, Faculty of Mining and Metallurgy, Yazd, Iran

(*Received February 05, 2015, Revised March 07, 2016, Accepted April 28, 2016*)

Abstract. The jointed rock mass behavior often plays a major role in the design of underground excavation, and their failures during excavation and in operation, are usually closely related to joints. This research attempts to evaluate the effects of two basic geometric factors influencing tunnel behavior in a jointed rock mass; joints spacing and joints orientation. A hybridized indirect boundary element code known as TFSDDM (Two-dimensional Fictitious Stress Displacement Discontinuity Method) is used to study the stress distribution around the tunnels excavated in jointed rock masses. This numerical analysis revealed that both the dip angle and spacing of joints have important influences on stress distribution on tunnel walls. For example the tensile and compressive tangential stresses at the boundary of the circular tunnel increase by reduction in the joint spacing, and by increase the dip joint angle the tensile stress in the tunnel roof decreases.

Keywords: boundary element method; dip; spacing; joint; tunnel

1. Introduction

Jointed rock masses are mainly found during underground excavation. Most failures in underground openings, during excavation and in operation, are reported to be closely related. Study of tunnel stability in jointed rock masses is of great significance to rock engineering, especially in tunneling and underground space development. Joints usually occur in sets which are more or less parallel and regularly spaced and also joint sets have different directions. In acute conditions, interaction between joints and tunnel stability may end in disasters. Performing model test and numerical analysis is a popular way to investigate the deformation and failure features of tunnel. Goodman et al. (1972) tested the behavior of tunnel deformation in jointed rock mass by using the scaled model test. Bieniawski (1974) presented the impacts of spacing and dip of joints in the strength of rock mass in underground excavation in rock mass classification RMR. To find out the impacts of the properties of joints in a rock mass on the stability of a tunnel which is excavated in the rock mass, Yeung and Leong (1997) performed a parametric study by using two-dimensional discontinuous deformation analysis (DDA). Button et al. (2006) conducted a research on the impacts of layering orientation in the general behavior and displacement of tunnel wall by using

*Corresponding author, M.Sc. in Rock Mechanics,
E-mail: Nooraddin.Nikadat@gmail.com, n.nikadat@stu.yazd.ac.ir
[a] Associate Professor, Ph.D., E-mail: Mohammad.Fatehi@gmail.com

Copyright © 2016 Techno-Press, Ltd.
 ISSN: 2005-307X (Print), 2092-6219 (Online)

district element method. To analyze the stability of rock blocks around a tunnel, Song et al. (2001) made use of a three-dimensional statistical joint modeling technique and concluded that the displaced blocks happened more repeatedly by increasing the joint persistence degree of scatter in joint set orientation and volumetric frequency of joints. Jia and Tang (2008) tried to find out the effect of joints orientation on tunnel stability by using a numerical method (RFPA). Palassi and Asadollahi (2007) in a study by using discrete element method investigated the impact of joint orientation in tunnel supporting system. Shou (2006) applied the 3D boundary element method to find out influences of the weak zone close to the tunnel. Goricki et al. (2005) studied about the impacts of foliations orientation on displacement around tunnels and concluded that the foliation does not have an influence on the displacement if its dip is 0 or 90° and also is liken to one of the major stresses. Besides, normal displacement is more, compared to shear displacement, in small dips. He also mentioned that shearing displacement has critical importance in joint dips of 40 to 80°. Jiang et al. (2006) presented a multiple system for analyzing the characteristics of geometrical distribution of rock joints, and mentioned the relationship between deformation behavior and fractal dimension and orientation of joint sets based on fractal analysis and numerical simulation of underground opening in the jointed rock mass.

Boundary element method has widely been for the stress analysis around underground opening. Crouch and Starfield (1983) presented the direct and indirect boundary element approaches for stress analysis in solid mechanics. The indirect boundary element method is further subdivided into Fictitious Stress Method (FSM) and Displacement Discontinuity Method (DDM), both of which can then be used in an effective way for solving elastostatic boundary value problems (BVP). FSM is more appropriate for stress and displacement analyses of BVP with stress boundary conditions and in continuous environments (Fatehi Marji and Manouchehrian 2010). Higher order DDM is more suitable for solving BVPs (Boundary Value Problems) with displacement boundary conditions and where discontinuities and cracks are introduced in the elastic body (Fatehi Marji and Hosseini-Nasab 2005, Fatehi and Hajibagherpour 2008, Fatehi Marji 2014, Ritz et al. 2012). In this study a hybridized indirect boundary element method (incorporating both FSM and DDM) is adopted to analyze the stress distribution around circular opening excavated in jointed rock masses. This method is highly accurate for stress distribution analysis which considers the joints effect (Nikadat et al. 2015, Ahmadi et al. 2015, Ansari and HodHodi 2015, Mussavi et al. 2014). The main purpose of the current study is to find out the effects of various dip angle and spacing of layered joints on the stability of tunnel which is excavated in jointed rock mass. The aim is to offer an insight into the influences of joints distribution on the stability of underground openings via numerical modeling and concluded that the dip of joints have a profound effect on the tunnel behavior.

2. Boundary Element Method (BEM)

Boundary Element Method (BEM) only discretizes the boundary of region of interest. Then, a familiar or calculated solution of a simple singular problem (known as the main solution) is made use of to build up the numerical solution for the whole mass by satisfying the boundary condition at each boundary element. BEM solutions can be summarized as: (i) Boundary discretization with a limited number of elements; (ii) Approximation of the local solution at boundary elements through shape functions; (iii) Evaluation of boundary influence coefficients; (iv) Application of boundary conditions and solution of the linear system of algebraic equations; (v) Evaluation of

field variables inside the domain.

BEM methods can be classified into direct and indirect methods. In the direct formulation, there is a clear physical meaning for calculated deformation and stresses, while it has no explicit physical meaning for the displacements and tractions in the indirect formulation, they may be explained as fictitious source densities (Jing 2003). In indirect BEM, discontinuities are modeled by making this assumption that two opposite surfaces displace along the discontinuity plane. An alternative for discontinuity modeling is the Displacement Discontinuity Method (DDM) which is a version of dual indirect boundary element methods. This method which basically was introduced by Salamon (1968) and developed by Crouch and Starfield (1983) is originated in integrating the analytical solution of a constant displacement discontinuity over a finite line segment embedded within an infinite or semi-infinite elastic solid that can be orthotropic in properties. In the current research, a hybridized form of indirect BEM known as "two-dimensional fictitious stress displacement discontinuity method (TFSDDM code)" which is adopted to study the effect of joint spacing and joint dip on the stress distribution around tunnels.

3. A hybridized Two-dimensional Fictitious Stress Displacement Discontinuity Method (TFSDDM)

The hybridized fictitious stress displacement discontinuity method offers a semi analytical solution for the problem under investigation. The TFSDDM code which is a two-dimensional hybridized indirect boundary element code is developed in the current study. In this code, joint displacements are calculated by using displacement discontinuities. Then through using the fictitious stress method (FSM), the impact of joints on the distribution of stress on the tunnel wall and within the rock mass is obtained. The formulation of FSM is developed based on the definitions shown in Fig. 1 by taking the fictitious stress components, P_x and P_y, into account at the center of a typical boundary element in x and y directions, respectively (Crouch and Starfield 1983).

The displacements in a two-dimensional isotropic elastic solid considering a general potential function, $f(x,y)$ can be written as

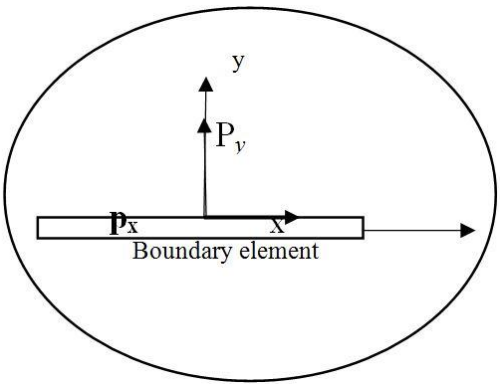

Fig. 1 A boundary element with shear and normal fictitious stress components P_x and P_y in x and y directions, respectively (Crouch and Starfield 1983)

$$u_x = \frac{P_x}{2G}[(3-4v)f - yf_y] + \frac{P_y}{2G}[-yf_x]$$
$$u_y = \frac{P_x}{2G}[-yf_x] + \frac{P_y}{2G}[(3-4v) - yf_y] \quad (1)$$

and the stresses are

$$\sigma_{xx} = P_x[(3-2v)f_x + yf_{xy}] + P_y[2vf_y + yf_{yy}]$$
$$\sigma_{yy} = P_x[-(1-2v)f_x - yf_{xy}] + P_y[2(1-v)f_y - yf_{yy}] \quad (2)$$
$$\sigma_{xy} = P_x[2(1-v)f_y + yf_{yy}] + P_y[(1-2v)f_x - yf_{xy}]$$

where G is shear modulus, υ poison ration, $f(x, y)$ is the potential function, u_x and u_y are displacement in X and Y direction.

$$f(x,y) = \frac{-1}{4\pi(1-v)}\Big[y\left(tan^{-1}\frac{y}{x-a} - tan^{-1}\frac{y}{x+a}\right) - (x-a)\,ln\sqrt{[(x-a)^2+y^2]} + (x+a)ln\sqrt{[(x+a)^2+y^2]}\Big] \quad (3)$$

and f_x, f_y, f_{xy}, etc are the derivatives of this function given in appendix A for completeness (Crouch and Starfield 1983). In FSM, the boundary of any boundary value problem (BVP) can be discretized into a number of finite boundary elements as shown in Fig. 2.

Taking the boundary conditions, b_s^i and b_n^i into account, a general system of algebraic equations can be obtained for determining the fictitious stress components P_s^j and P_n^j so that the displacements and stresses along the boundary and within the domain of the problem can be estimated by Eqs. (1) and (2), respectively.

$$b_s^i = \sum_{j=1}^{N} C_{ss}^{ij} P_s^j + \sum_{j=1}^{N} C_{sn}^{ij} P_n^j$$
$$b_n^i = \sum_{j=1}^{N} C_{ns}^{ij} P_s^j + \sum_{j=1}^{N} C_{nn}^{ij} P_n^j \qquad (i = 1 \ \ to \ \ N), (J = 1 \ \ to \ \ N) \quad (4)$$

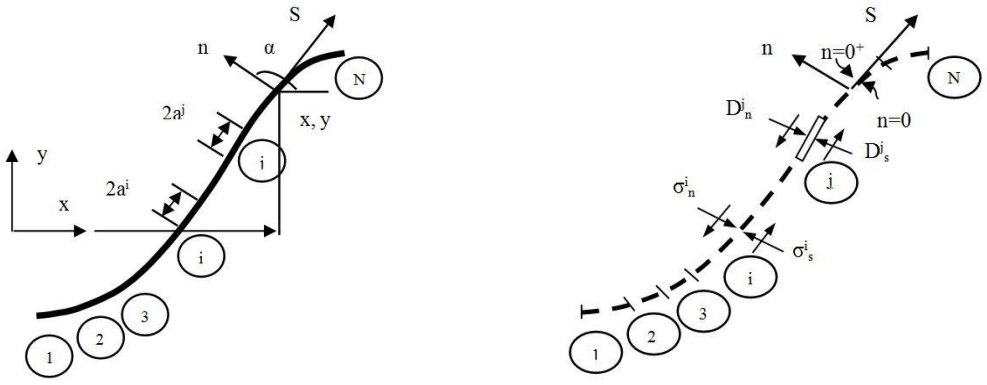

(a) (b)

Fig. 2 Representation of a crack by N elemental displacement discontinuities (Crouch and Starfield 1983)

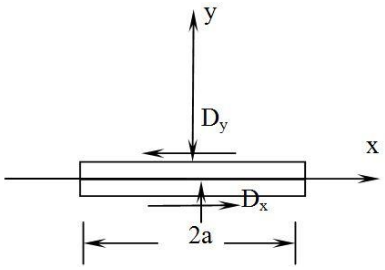

Fig. 3 Constant element displacement discontinuity element (Crouch and Starfield 1983)

where C_{ss}^{ij}, C_{sn}^{ij}, etc. are the corresponding influence conditions (Crouch and Starfield 1983). In the hybridized fictitious stress displacement discontinuity method which is utilized in the present study to model the discontinuities or joints in a rock mass embodying an underground space, the displacement discontinuity method is used. The displacement discontinuity method is based on the analytical solution of the problem of a constant displacement discontinuity, or dislocation, over a finite line segment in an infinite elastic body like what is presented in Fig. 3.

The elemental displacement discontinuities are explained with regard to the local coordinates *s* and *n*. The normal component of displacement discontinuity at the *j-th* segment is known as D_n^j the tangential, or shear, component is named D_s^j. As a result, the permanent element displacement discontinuities D_s and D_n can be written as follows

$$\begin{aligned} D_s^j &= u_s^{j-} - D_s^{j+} \\ D_n^j &= u_n^{j-} - D_n^{j+} \end{aligned} \tag{5}$$

In these definitions, u_s^j and u_s^j refer to the shear (s) and normal (*n*) displacements of the *j*-th segment of the crack. The superscripts + and – respectively mark the positive and negative surfaces of the crack (Crouch and Starfield 1983).

The displacements and stresses in a two-dimensional isotropic elastic solid can be written as

$$\begin{aligned} u_x &= D_x\left(2(1-v)f_{,y} - yf_{,xx}\right) + D_y\left(-(1-2v)f_{,x} - yf_{,xy}\right) \\ u_y &= D_x\left((1-2v)f_{,x} - yf_{,xy}\right) + D_y\left(2(1-v)f_{,y} - yf_{,yy}\right) \end{aligned} \tag{6}$$

$$\begin{aligned} \sigma_{xx} &= 2GD_x\left(2f_{,xy} + yf_{,xyy}\right) + 2GD_y\left(f_{,yy} + yf_{,yyy}\right) \\ \sigma_{yy} &= 2GD_x\left(-yf_{,xyy}\right) + 2GD_y\left(f_{,yy} - yf_{,yyy}\right) \\ \sigma_{xy} &= 2GD_x\left(f_{,yy} + yf_{,yyy}\right) + 2GD_y\left(-yf_{,xyy}\right) \end{aligned} \tag{7}$$

f_x, f_y etc are the partial derivatives of the single harmonic functions $f(x, y)$ given in Eq. (3). The partial derivatives, $f_{,yyy}$ and $f_{,xyy}$ are also given in Appendix A. Two types of boundary conditions i.e. the shear and normal stresses boundary conditions $\sigma_{si} = (\sigma_{si})_0$, $\sigma_{ni} = (\sigma_{ni})_0$ are generally taken into acount in plane elasticity problems, and the shear and normal displacements boundary conditions $u_{si} = (u_{si})_0$, $u_{ni} = (u_{ni})_0$, in which $(\sigma_{si})_0$, $(u_{si})_0$, etc. are the corresponding stress and displacement values determined at the boundary of the problem. Hence, the quantities b_s^i, and b_n^i can stand for the familiar boundary values of stress and displacement and C_{ss} (i, j), etc. are

the corresponding influence coefficient.

$$\left\{\begin{array}{l} {}^{i}b_s = \sum_{j=1}^{N} {}^{ij}C_{ss}\,{}^{j}D_s + \sum_{j=1}^{N} {}^{ij}C_{sn}\,{}^{j}D_n \\ {}^{i}b_n = \sum_{j=1}^{N} {}^{ij}C_{ns}\,{}^{j}D_s + \sum_{j=1}^{N} {}^{ij}C_{nn}\,{}^{j}D_n \end{array}\right\} \; i = 1\,to\;\; N \tag{8}$$

The discretized form of displacement discontinuity equation can be formed and finally a system of 2(N = N) algebraic equation in 2(N = N) unknown displacement discontinuity components is obtained as

$$\begin{bmatrix} {}^{i}\sigma_s \\ {}^{i}\sigma_n \end{bmatrix} = \begin{bmatrix} {}^{ij}A_{ss} & {}^{ij}A_{sn} \\ {}^{ij}A_{ns} & {}^{ij}A_{nn} \end{bmatrix} \begin{bmatrix} {}^{j}D_s \\ {}^{j}D_n \end{bmatrix} \tag{9}$$

$$\begin{bmatrix} {}^{i}U_s \\ {}^{i}U_n \end{bmatrix} = \begin{bmatrix} {}^{ij}B_{ss} & {}^{ij}B_{sn} \\ {}^{ij}B_{ns} & {}^{ij}B_{nn} \end{bmatrix} \begin{bmatrix} {}^{j}D_s \\ {}^{j}D_n \end{bmatrix} \tag{10}$$

where A_{ss} (i, j) *and* B_{ss} (i, j) are the boundary influence coefficient.

In this research, the joints are firstly modeled by considering a linear elastic behavior, and for final modeling, Mohr–Coulomb plastic criterion is used after the rock failure. The effective parameters on the joint behavior are cohesion, friction angle, tensile stress and joint's normal and shear stiffness; therefore the plastic–elastic rocks feature can be simulated based on the plane strain (thickness of the discontinuity is not important). Joints can show three behaviors according to the following conditions

$$\sigma_s = \sigma_n = 0 \qquad \text{(Open joints)} \tag{11}$$

$$\begin{aligned} \sigma_n &= K_n D_n \\ \sigma_s &= K_s D_s \end{aligned} \qquad \text{(Closed joints)} \tag{12}$$

$$\begin{aligned} |\sigma_s| &= \sigma_n \tan\phi + c \\ \sigma_n &= K_n D_n \end{aligned} \qquad \text{(Sliding joints)} \tag{13}$$

where K_n and K_s are joint normal and joint shear stiffness's respectively, σ_n and σ_s are normal and shear stresses, c is joint cohesion and φ is the joint friction angle. A joint can be described as a long, thin crack with the compressible modeled filling. Fig. 4 presents the two springs with the normal and shear stiffness, K_n and K_s, respectively for modeling the linear elastic joints. According to Fig. 4 the relations between the stresses, strains and displacement discontinuities may be written as

$$\begin{aligned} \sigma'_{yy} &= E_0 e'_{yy} = -E_0 \frac{D'_y}{h} \\ \sigma'_{xy} &= 2G_0 e'_{xy} = -G \frac{D'_x}{h} \end{aligned} \tag{14}$$

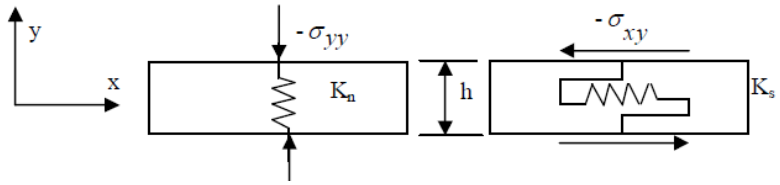

Fig. 4 Linear elastic joint modeling (Crouch and Starfield 1983)

$$\begin{aligned}\sigma'_n &= -K_n D'_n \\ \sigma'_s &= -K_S D'_s\end{aligned} \tag{15}$$

In which the prime sign stands for the parameters of a specific joint element and σ_{yy} and σ_{xy} are induced stresses, e_{yy} is the strain of the spring at the *y* direction, E_0 and G_0 young and shear's modulus and *h* is element thickness.

Sliding and separation of the joint may be controlled by Mohr-Coulomb criterion as

$$|\sigma_s| = \sigma_n \tan\phi + c \tag{16}$$

In which Shear stress on the joints should not overpass the value obtained in Eq. (16) otherwise, it may result in sliding and fracture. Sliding along the joint is in linear mode and can be modeled in incremental mode. The initial stress gradually gets to zero through several steps. The number of incremental stress on joints is showed by *k* symbol.

$$\left.\begin{aligned}\frac{-k}{K}({}^{i}\sigma_s)_0 &= \sum_{j=1}^{N} A_{ss}^{ij\ j} X_s^{(k)} + \sum_{j=1}^{N} A_{sn}^{ij\ j} X_n^{(k)} \\ \frac{-k}{K}({}^{i}\sigma_n)_0 &= \sum_{j=1}^{N} A_{ns}^{ij\ j} X_s^{(k)} + \sum_{j=1}^{N} A_{nn}^{ij\ j} X_n^{(k)}\end{aligned}\right\} 1 \le i \le M \tag{17}$$

The increase/iterative load technique may be utilized for the nonlinear analysis of a problem

$$\left.\begin{aligned}\overset{i}{\sigma'_S} &= \sum_{j=1}^{N} (\overset{ij}{A_{ss}}\ \overset{j}{X_s} + \overset{ij}{A_{sn}}\ \overset{j}{X_n}) \\ \overset{i}{\sigma'_n} &= \sum_{j=1}^{N} (\overset{ij}{A_{ns}}\ \overset{j}{X_s} + \overset{ij}{A_{nn}}\ \overset{j}{X_n})\end{aligned}\right\} \left(i = 1\ \ to\ \ N\right) \tag{18}$$

$$\left.\begin{aligned}\overset{j}{X}_s &= \overset{j}{P}_s \\ \overset{j}{X}_n &= \overset{j}{P}_n\end{aligned}\right\}\ 1 \le j \le M \tag{19}$$

$$\left.\begin{aligned}\overset{j}{X}_s &= \overset{j}{D'}_s \\ \overset{j}{X}_n &= \overset{j}{D'}_n\end{aligned}\right\}\ M+1 \le j \le N \tag{20}$$

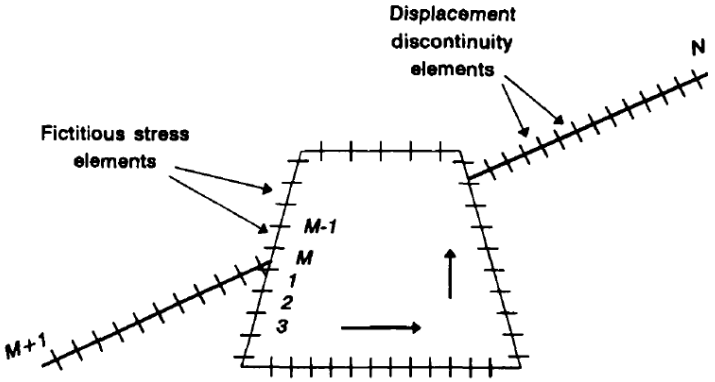

Fig. 5 Boundary element modeling of an underground opening intersected by a fault (i.e., a single discontinuity) (Fotoohi and Mitri 1996)

For modeling a tunnel in a jointed rock mass, FSM is used to model the tunnel boundary and the displacement discontinuity method is used to model the discontinuities or joints. As an example, Fig. 5 shows that if one has a total *N* boundary elements in a way that M elements model the tunnel boundary (by using FSM), then *N-M* elements model the joints (by using DDM).

Hence, with hybridizing the two mentioned methods, the impact of the discontinuity (e.g., dips and spacing) on the stress distribution around the tunnel can be obtained (Fotoohi and Mitri 1996). This procedure may be formulated as

$$\left.\begin{aligned} -({}^{i}\sigma_s)_0^{\infty} &= K_s^i X_s^i + \sum_{j=1}^{N} A_{ss}^{ij} X_s^j + \sum_{j=1}^{N} A_{sn}^{ij} X_n^j \\ -({}^{i}\sigma_n)_0^{\infty} &= K_n^i X_n^i + \sum_{j=1}^{N} A_{ns}^{ij} X_s^j + \sum_{j=1}^{N} A_{nn}^{ij} X_n^j \end{aligned}\right\} M+1 \le i \le N \tag{21}$$

$$\left.\begin{aligned} -({}^{i}\sigma_s)_0^{\infty} &= \sum_{j=1}^{N} A_{ss}^{ij} X_s^j + \sum_{j=1}^{N} A_{sn}^{ij} X_n^j \\ -({}^{i}\sigma_n)_0^{\infty} &= \sum_{j=1}^{N} A_{ns}^{ij} X_s^j + \sum_{j=1}^{N} A_{nn}^{ij} X_n^j \end{aligned}\right\} 1 \le i \le M \tag{22}$$

The most distinctive characteristic of TFSDDM code which makes it unique compared to other kinds of numerical codes is that since two different methods are used for modeling of joints and geometrical shapes of tunnels, the intersection between joints and tunnels are modeled more accurately and also the code illustrates a joint influence on the whole value of stress distribution around tunnel in a better way. The influence of each element on the other elements is presented in the influence coefficient matrix. It can deal with singular points very well and provide reasonably good results. The TFSDDM Program's algorithm is schematically shown in Fig. 6. In this figure, Ɛ is the error rate which equals 0.1. The obtained convergence is compared to the allowed convergence and if it is less than 0.1, the circulation is repeated.

The whole algorithm is controlled by stress release steps which were presented at the beginning.

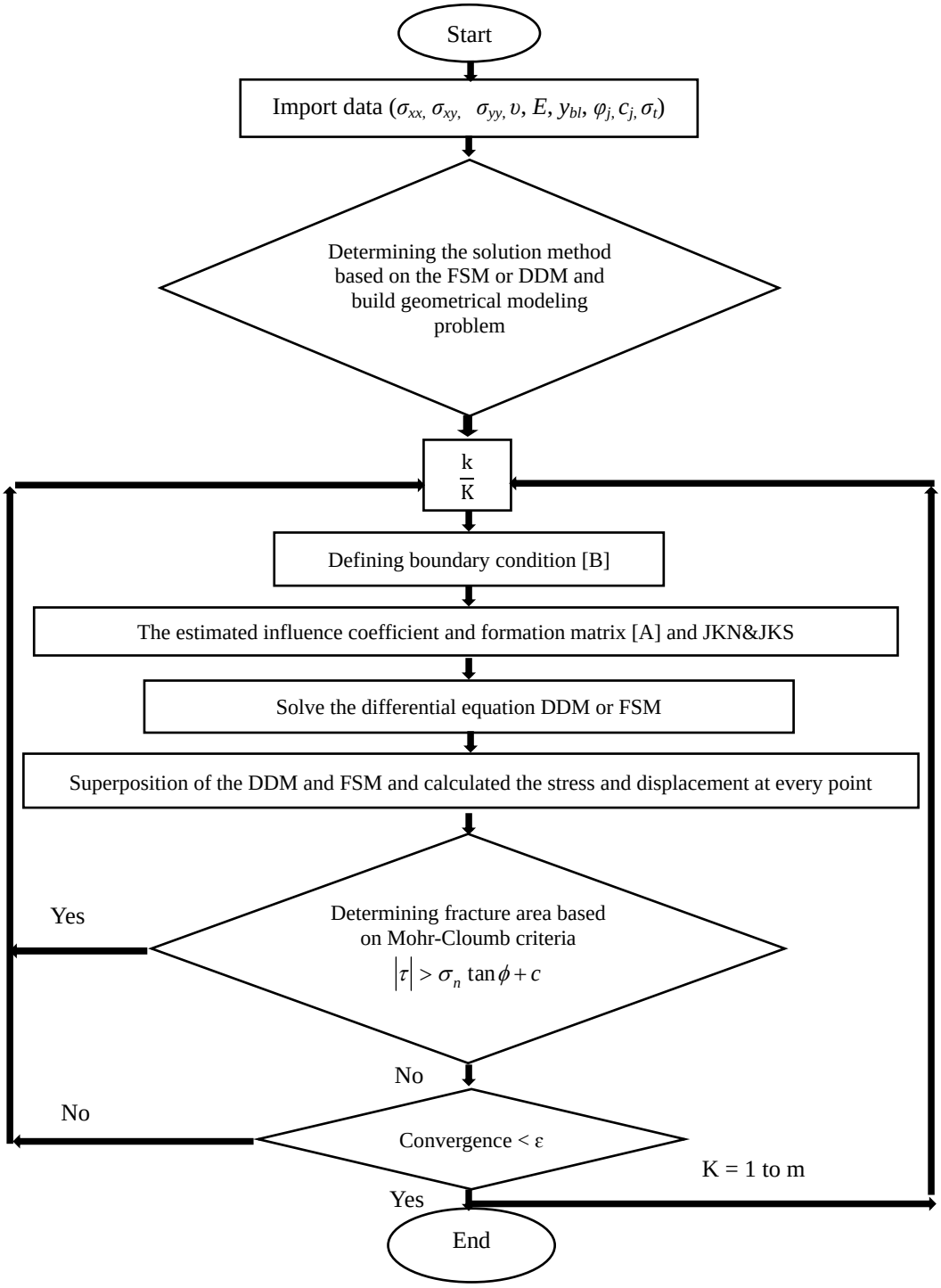

Fig. 6 The TDDFSM algorithm

If all steps are passed and the whole element is yielded, the problem is solved and it is schematic of the original algorithm.

4. Effects of joint spacing on the stress distribution

One of the significant geometrical characteristics of joint's geometrical that influences the rock mass behavior is Joint spacing. When joint spacing increases, the rock mass behavior gets closer to the intact rock behavior. Effect of joint spacing on the stress distribution in jointed rock mass surrounding a circular tunnel is studied by the two-dimensional hybridized fictitious stress displacement discontinuity method (TFSDDM) which in this study is developed according to the indirect boundary element method explained by Crouch and Starfield (Crouch and Starfield 1983).

In the present study, the joints are firstly modeled by considering a linear elastic behavior and after the failure, they are modeled according to Mohr–Coulomb plastic criteria. The Joints behavior are modeled based on the cohesion ,friction, tensile stress, joint normal and joint shear stiffness; therefore characteristics of the plastic–elastic rocks can be simulated based on the plane strain rocks (thickness of the discontinuity is not important). In spite of the fact that the Effect of Mechanical parameters on the behavior of the joint is of paramount importance, in this research the mechanical parameter for all the modes is the same and only the effect of the geometrical parameters is probed. The most unique feature of this code, which makes it totally different from other kinds of numerical codes is that since two different methods are used for modeling the joint and geometrical shape of the tunnel, the intersection between joint and tunnel are modeled more accurately and also illustrates the joint influence on the whole amount of stress distribution around tunnel in a better way.

Fig. 7 presents a schematic view of a circular tunnel at depth H from the ground surface. All models which are utilized in this study are considered to be under uniaxial stress condition and Mohr-Coulomb criterion is used for joint sliding.

The geo-mechanical properties of the rock mass which were used in this study are shown in

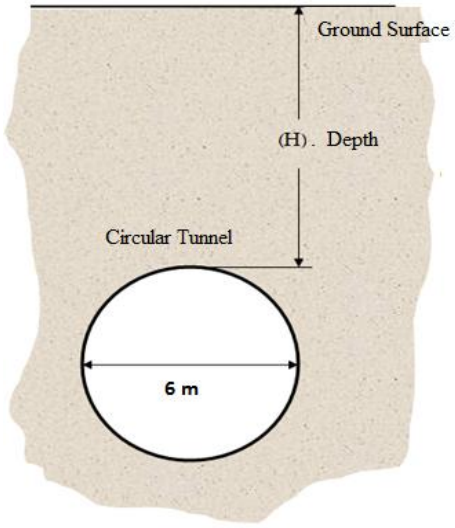

Fig. 7 Geometrical shape of the model

Table 1. In this table the normal and shear joint stiffness are symbolized as JKN (in MPa/m) and JKS (in MPa/m), respectively. The tensile strength, (Ten Str (MPa)) of the jointed rock is taken as zero. The cohesion (C_j (MPa)) and friction angle (φ_j in degrees (°)) for joints are presented in the table. The young modulus E (MPa) and Poisson's ratio ν are also considered for the jointed rock mass.

Statement of the problem is modelled by considering a circular tunnel in a continuous elastic rock mass with the Young modulus, E = 37.5 GPa and Poisson's ratio, v = 0.25 at a considerable depth below the surface. The analytical solution to this problem can be acquired from the Kirsch solution. This problem is solved by BEM codes (TFSDDM) and the results are presented in Fig. 8.

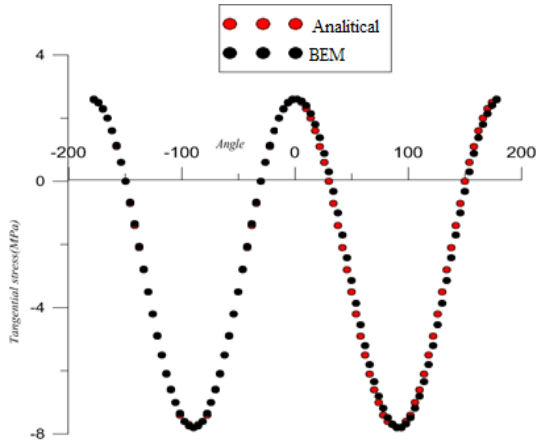

Fig. 8 The compared TFSDDM code and Analytical method (Nikadat 2014)

Table 1 Geo-mechanical parameters of a typical jointed rock mass

JKN (MPa/m)	JKS (MPa/m)	Ten Str (MPa)	C_j (MPa)	Θ_j (°)	E (Mpa)	N
20000	10000	0	1.5	33	37500	0.25

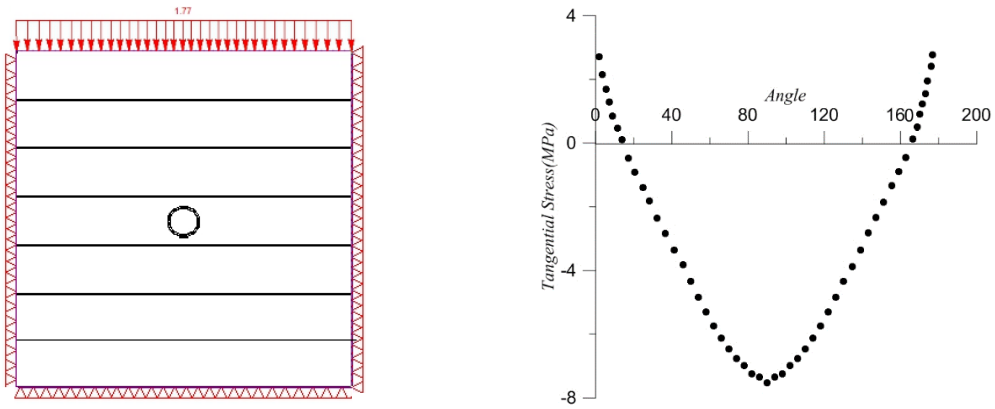

(a) Geometrical shape of the model (b) Stress distribution Using BEM

Fig. 9 Stress distribution at a circular tunnel boundary considering Joint spacing 10 m

As shown in this figure the results obtained by BEM are much closer to the analytical solution compared to the results obtained by Kirsch method (exact solution) (Nikadat 2014).

The geometrical models of the problem with similar stress distribution graphs for a surrounded rock mass containing parallel joints of different spacing are presented in the following figures.

Fig. 9 shows the geometry and tangential stress distribution around a circular tunnel for a rock mass with joint spacing of 10 meters. In this case, there is no intersection between the joints and tunnel walls. So, the BEM stress distribution graphs are similar to that of analytical solution which was presented by Kirsch.

In Fig. 10 joint spacing is reduced to 7 meters so that one of the parallel joints intersects the circular tunnel at right angle. The tangential stress distribution around the tunnel is calculated by the BEM method. This result is very accurate because the intersection of joint with the tunnel boundary can be visualized by this method. In this case, compared to the previous model, the tension stress in the roof and the compressive stress in the wall increase.

The joint spacing in Fig. 11 is reduced to 5 meters. Again one of the joints intersects the tunnel boundary at 90 degrees angle. Fig. 11 presents more tensile stress at tunnel roof and gives a picture of the intersection of the joint with tunnel boundary at point 1. In this case, the tensile stress in the roof and compressive stress in the wall increases.

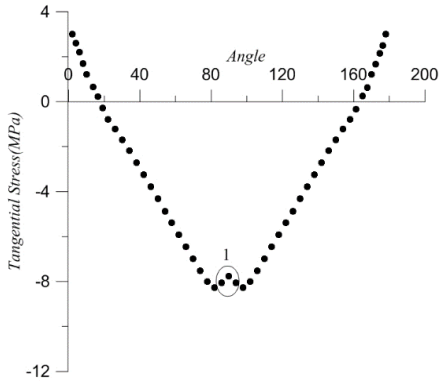

Fig. 10 Stress distribution at a circular tunnel boundary considering Joint spacing 7 m

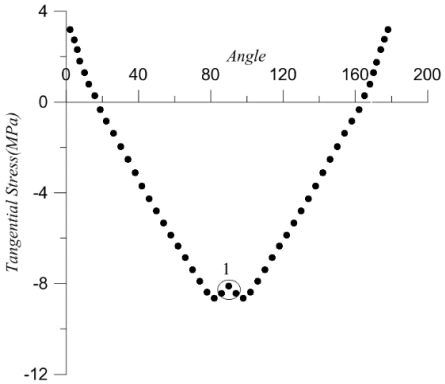

Fig. 11 Stress distribution at a circular tunnel boundary considering Joint spacing 5 m

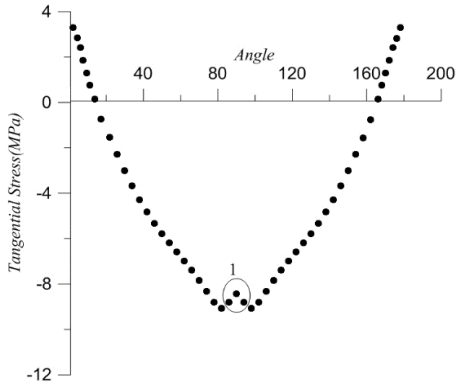

Fig. 12 Stress distribution at a circular tunnel boundary considering Joint spacing 3.5 m

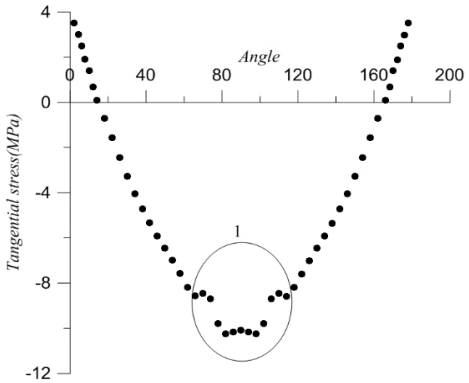

Fig. 13 Stress distribution at a circular tunnel boundary considering Joint spacing 2 m

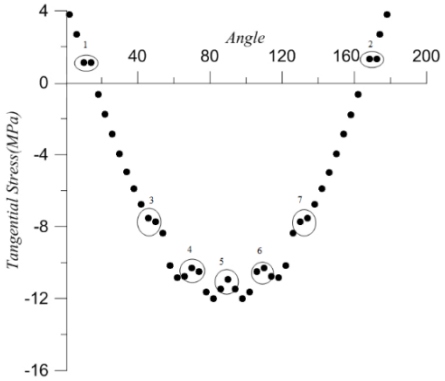

Fig. 14 Stress distribution at a circular tunnel boundary considering Joint spacing 1 m

In Fig. 12 where the joint spacing is reduced to 3.5 meters, one joint intersects the tunnel wall and the other two get very close to the roof and bottom of the tunnel. As a result, one layer with a width of less than 0.5 meter may be assumed in the tunnel roof. Fig. 12 show the BEM results in which the tensile stress is more at the tunnel roof and the joint intersection with tunnel boundary is

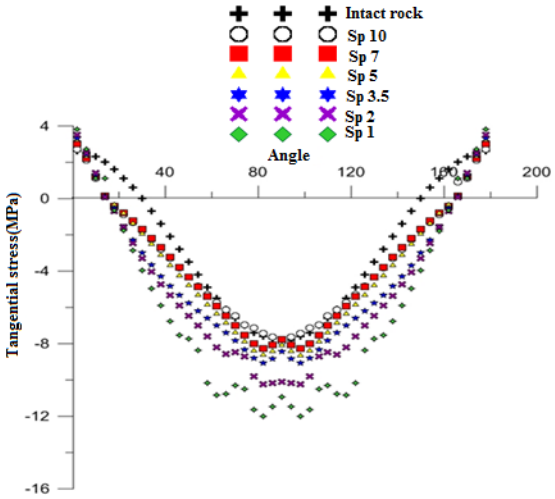

Fig. 15 Comparison of stress distribution diagrams for various spacing

Table 2 Compression stress between various spacing

	Kirsch	Intact	Sp 10	Sp 7	Sp 5	Sp 3.5	Sp 2	Sp 1
Wall	-7.78	-7.8	-7.9	-8.28	-8.66	-9.08	-10.25	-12.01
Roof	2.59	2.6	2.7	3	3.18	3.34	3.5	3.8

shown by point 1.

In Fig. 13, the joint spacing is further reduced to 2 meters so that two joints intersect the tunnel wall and two joints are tangent to both roof and bottom of the circular tunnel. The BEM results are given in Fig. 13 which shows that mo joints have intersected the tunnel boundary at section 1 (the region shown by the ellipse).

In Fig. 14 joint spacing is reduced to about 1 meter. In this case 5 joints have intersected the tunnel wall and two joints are tangent to the roof and bottom of the tunnel. Fig. 14 shows the stress distribution obtained by BEM. In this figure, all intersection points and tangents to the boundary

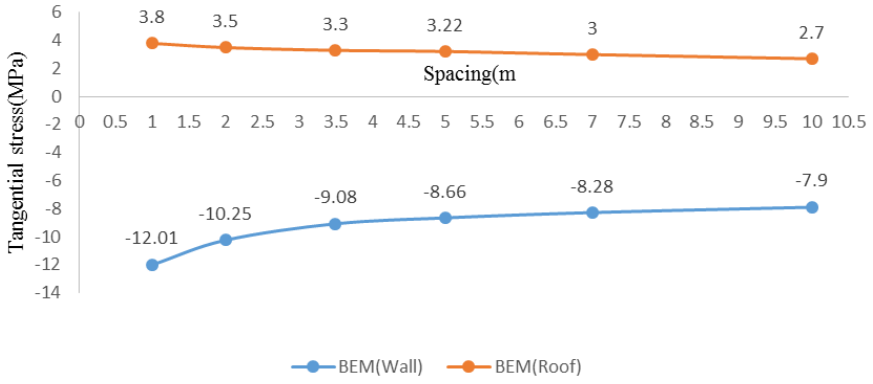

Fig. 16 Stress distribution on the wall and roof

are distinguished by the method which is presented by closed regions on the graph. The tensile and compressive tangential stresses around the boundary of the circular tunnel increase as the joint spacing decreases.

In order to make a comparison, all spacing graphs are given in a chart in Fig. 15. According to it, by increasing the joints spacing, stress distribution on the wall decreases.

The stress distribution at the tunnel boundary (with decrease in the joint spacing) obtained by BEM is presented in Table 2.

Graphs derived from this table are shown in Fig. 16.

It can be concluded that with increase in joint spacing, tangential stress around the tunnel (especially at roof) decreases which is clearly apparent in this method.

5. Effects of joints dips on the stress distribution around tunnel

One of the most important geometrical features of joint which can influence the rock mass behavior is dip angle of joints. When orientation of the principal stress and joints are similar, the rock mass behavior approaches the intact rock behavior. The influence of joint dip angles on the stress distribution at the boundary of a circular tunnel excavated in a jointed rock mass is also studied by the BEM. In this section that the effect of the joint dip is studied the conditions are similar to those given in Section 4, but the joint spacing is kept constant (3.5 meters) and only joint dip angle changes.

The effect of joint dip angle zero (horizontal joints) on the tangential stress distribution around a circular tunnel is already presented in Fig. 12. In this state, the compressive stress at the wall and tensile stress in the roof are in maximum.

In the model shown in Fig. 17, two joints have intersected the tunnel boundary and the joint dip angle is 30 degrees. Fig. 17 shows the stress distribution at the tunnel boundary obtained by BEM (TFSDDM code). This figure shows that the stress is released at the intersection points and stress distribution diagram is cluttered.

In Fig. 18, the joint dip angle is further increased to 60 degrees and again two joints intersect the tunnel boundary. In this case, since the joint dip angle increases, the displacements changes

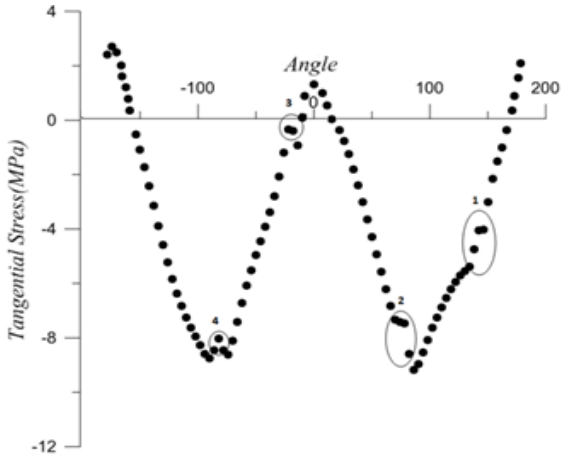

Fig. 17 Stress distribution at a circular tunnel boundary considering Joint Dip 30 degree

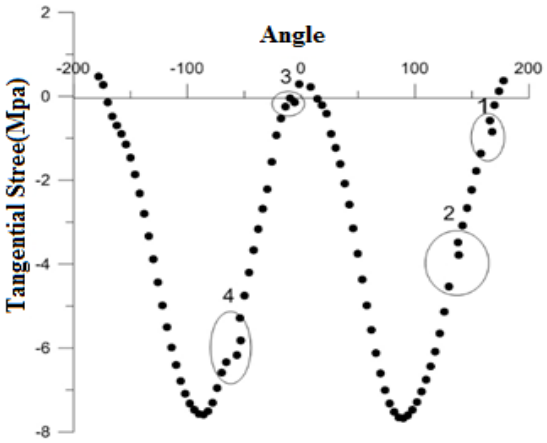

Fig. 18 Stress distribution at a circular tunnel boundary considering Joint Dip 60 degrees

from normal to shear as a result, changes in stress distribution at intersect point of joint and tunnel wall are less than those of previous case. Fig. 18 also shows that tensile stress in roof and bottom is decreased.

In Fig. 19 the joint dip angle reaches to 90 degrees (vertical joints). Fig. 19 shows the tangential stress distribution at the tunnel boundary for BEM. This figure shows that the tensile stress at the tunnel roof and bottom is completely vanished. Therefore, in this stress graphs are getting more compact comparing to the graphs shown before for non-vertical joints. The minimum tensile stress in the roof and the compressive stress in the walls happened in this case. The shear displacement in the roof increases with increase in joint dip angle. As a result the tensile stress decreases.

Effect of joint dip angle on the tangential stress distribution at the circular tunnel boundary (obtained by BEM) are given in Table 3. From the figure, we can see that dip angle has significant effect on the stress distribution of tunnel walls.

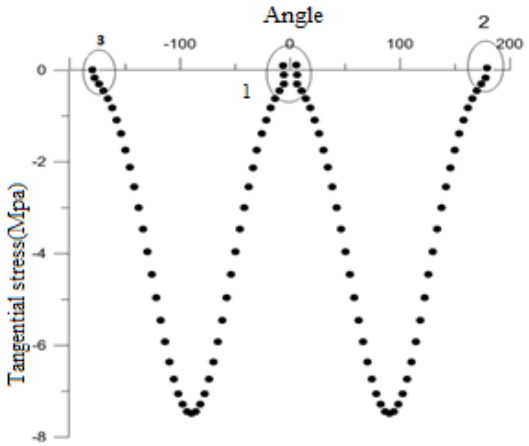

Fig. 19 Stress distribution at a circular tunnel boundary considering Joint Dip 90 degrees

Table 3 Stress comparison between various joint dips

	0 Degree	30 degree	60 degree	90 degree
Floor	3/5	1/1	0/19	-0/17
the right wall	-9/18	-9/08	-7/67	-7/49
Roof	3/5	2/7	0/48	-0/17
the left wall	-9/18	-8/76	-7/59	-7/49

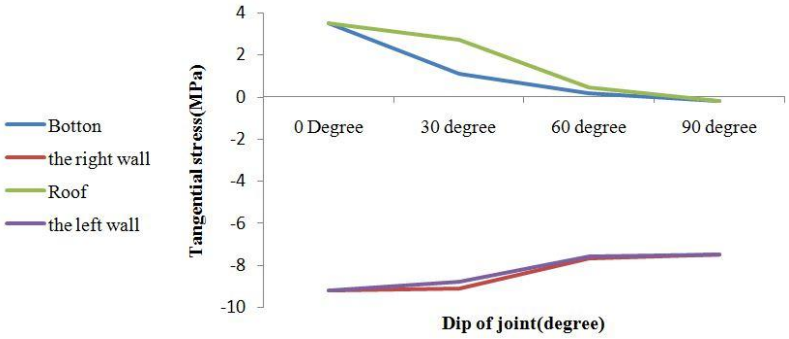

Fig. 20 Stress distribution on the wall an 4 point in different dip angle of joints

The effect of joint dip angle on the stress distribution at the circular tunnel boundary is estimated numerically by using BEM (TFSDDM) at 4 point on the tunnel boundary is illustrated graphically in Fig. 20. These graphs show that the tangential stress is decreased as the joint dip angle is increased and the numerical results getting closer to each other as the dip angle increases.

According to graphs, when the roof is in the highest state of tensile stress, the dip is zero. In the case of joints dip being 90°, there is minimal stress concentration and no tension stress is created in the roof and bottom area and the graph is more intensive.

6. Conclusions

In this study, the influence of joint geometrical parameters on the stress distribution on tunnel wall in jointed rock mass is investigated by the indirect boundary element method called two-dimensional hybridized fictitious stress displacement discontinuity method (TFSDDM). This analysis indicated that both the dip angle and joint spacing have significant impact on the stress distribution around the tunnel. Based on these analyses, the following conclusions were drawn:

- The results obtained by BEM in intact rock are much closer to the analytical solution (Exact solution). It should be noted that as BEM is a semi-analytical method, that reduces is one dimension of the problem and can take into account the effects of infinite boundaries. Truncating the boundary of model increases error chance, but in boundary element method unlike other numerical methods there is no need to truncate the boundary of the model and as a result it has high accuracy.
- The BEM results are very accurate, because the intersection of joint with the tunnel boundary can be visualized by this method. BEM can discretize the tunnel boundary and

the joints separately; therefore the intersection points can be visualized.

- The rock mass behavior approaches to that of intact rock behavior when the orientation of the principal stress and joints are the same (in the case of vertical joints).
- The tensile and compressive tangential stresses at the boundary of the circular tunnel are increasing as the joint spacing decreases
- By increasing the dip joint angle the tensile stress in the tunnel roof decreases.
- When the joint dip angle increases, the displacements changes from normal to shear, the tangential stress at tunnel boundary decreases.
- The tensile stress concentration at the roof and bottom of the tunnel is maximized when the dip angle of the joint is zero degree.
- The minimum tensile stress concentration is achieved when the joint dip angle is 90 degrees.

References

Ahmadi, N., Fatehi Marji, M. and Yarahmadi Bafghi, A. (2015), "Modeling the effect of faults on the tangential stress distribution around two adjacent tunnels using indirect boundary element method" *Proceedings of the 5th Iranian Mining Engineering Conference*, Tehran, Iran, October. [In Persian]

Ansari, H. and HodHodi, M. (2015), "Evaluation Stress around circular tunnel using analytical and numerical methods", *Proceedings of the 1st Technical Engineering Conference*, Tehran, Iran, December. In Persian]

Bieniawski, Z.T. (1974), "Geo-mechanics classification of rock masses and its application in tunneling", *Proceedings of the 3rd Congress of the International Society for Rock Mechanics*, (Volume 2), Washington, D.C., USA, pp. 27-32.

Button, E.A., Leitner, R., Poetsch, M. and Schubert, W. (2006), "Spatial relationships between discontinuity orientation and system behavior in underground excavations", *Golden Rocks*, **50**, 189-201.

Crouch, S.L. and Starfield, A.M. (1983), *Boundary Element Methods in Solid Mechanics*, George Allen & Unwin (Publishers) Ltd.

Fatehi Marji, M. (2014), "Numerical analysis of quasi-static crack branching in brittle solids by a modified displacement discontinuity method", *Int. J. Solids Struct.*, **51**(9), 1716-1736.

Fatehi Marji, M. and Hajibagherpour, A. (2008), "On the stability analysis of shallow tunnels in hard rocks by a hybridized Boundary Element/Finite Difference (BE/FD) Method", *Proceedings of the 6th International Symposium Rock Bolting in Mining, Injection Technology and Roadway Support Systems*, Mining Engineering Department, RWTH University; Aachen, Germany, May.

Fatehi Marji, M. and Hosseini-Nasab, H. (2005), "Application of higher order displacement discontinuity method using special crack tip elements in rock fracture mechanics", *Proceedings of the 20th World Mining Congress & Expo*, Tehran, Iran, November, pp. 699-704.

Fatehi Marji, M. and Manouchehrian, A. (2010), "Investigation of horizontal to vertical stress ratio (K) effect on displacement and stress concentration around underground Excavation by using BEM", *Proceedings of the 3rd Iranian Mining Engineering Conference*, Yazd University, Yazd, Iran, January.

Fotoohi, K. and Mitri, H. (1996), "Non-linear fault behavior near underground excavations –A boundary element approach", *Int. J. Numer. Anal. Meth. Geomech.*, **20**(3), 173-190.

Goodman, R.E., Heuze, H.E. and Bureau, G.J. (1972), "On modeling techniques for the study of tunnels in jointed rock", *Proceedings of the 14th Symposium on Rock Mechanics*, University Park, PA, USA, June, pp. 441-479.

Goricki, A., Button, A., Schubert, W., Markus, P. and Roland, L. (2005), "The Influence of Discontinuity Orientation on the Behavior of Tunnels", *Felsbau*, **23**(5), 12-18.

Jia, P. and Tang, C.A. (2008), "Numerical study on failure mechanism of tunnel in jointed rock mass", *Tunn. Undergr. Space Technol.*, **23**(5), 500-507.

Jiang, Y., Tanabashi, Y., Li, B. and Xiao, J. (2006), "Influence of geometrical distribution of rock joints on deformational behavior of underground opening", *Tunn. Undergr. Space Technol.*, **21**(5), 485-491.

Jing, L. (2003), "A review of techniques, advances and outstanding issues in numerical modelling for rock mechanics and rock engineering", *Int. J. Rock Mech. Min. Sci.*, **40**(3), 283-353.

Nikadat, N. (2014), "Investigating the effect of geometrical properties of discontinuity on stress distribution around underground opening using BEM and FEM", M.Sc. Thesis; Department of Mine Exploitation Engineering, Faculty of Mining and Metallurgy, Yazd, Iran. [In Persian]

Nikadat, N., Fatehi Marji, M. and Abdollahipour, A. (2015), "Numerical modelling of stress analysis around rectangular tunnels with large discontinuities (fault) by a hybridized indirect BEM", *J. Cent. South Univ.*, **22**(11), 4291-4299.

Mussavi, A., Fatehi Marji, M. and Lazemi, H. (2014), "Analysis of stresses and displacements around circular tunnel using indirect boundary element method", *Proceedings of the 1st Iranian Conference of Geotechnical Engineering*, Ardabil, Iran, October. [In Persian]

Palassi, M. and Asadollahi, P. (2007), "Tunnel design using continuum and discontinuum approaches and the effect of joint orientation on the design", *Electron. J. Geotech. Eng.*

Ritz, E., Mutlu, O. and Pollard, D.D. (2012), "Integrating complementarity into the 2D displacement discontinuity boundary element method to model faults and fractures with frictional contact properties", *Comput. Geosci.*, **45**, 304-312.

Salamon, M.D.G. (1968), "Two-dimensional treatment of problems arising from mining tabular deposits in isotropic or transversely isotropic ground", *Int. J. Rock Mech. Min. Sci.*, **5**(2), 159-185.

Shou, K. (2006), "Boundary element analysis of tunnelling through a weak zone", *J. Geoeng.*, **1**(1), 25-28.

Song, J., Lee, C. and Seto, M. (2001), "Stability analysis of rock blocks around a tunnel using a statistical joint modeling technique", *Tunn. Undergr. Space Technol.*, **16**(4), 341-351.

Yeung, M.R. and Leong, L.L. (1997), "Effects of joint attributes on tunnel stability", *Int. J. Rock Mech. Mining Sci.*, **34**(3-4), 348.e1-348.e18.

CC

Appendix A

Derivatives of the potential function $F(x, y)$ used in the formulation of fictitious stress method

$$f_x = \frac{-1}{4\pi(1-\nu)} \frac{x}{x^2+y^2}$$

$$f_y = \frac{-1}{4\pi(1-\nu)} \frac{y}{x^2+y^2}$$

$$f_{xy} = \frac{-1}{4\pi(1-\nu)} \frac{2xy}{(x^2+y^2)^2}$$

$$f_{xx} = -g_{yy} \frac{1}{4\pi(1-\nu)} \frac{x^2-y^2}{(x^2+y^2)^2}$$

Derivatives of the potential function $F(x, y)$ used in the formulation of displacement discontinuity method

$$f_{,x} = \frac{+1}{4\pi(1-\nu)} \left[ln\sqrt{(x-a)^2+y^2} - ln\sqrt{(x+a)^2+y^2} \right]$$

$$f_{,y} = \frac{-1}{4\pi(1-\nu)} \left[tan^{-1}\frac{y}{x-a} - tan^{-1}\frac{y}{x+a} \right]$$

$$f_{,xy} = \frac{+1}{4\pi(1-\nu)} \left[\frac{y}{(x-a)^2+y^2} - \frac{y}{(x+a)^2+y^2} \right]$$

$$f_{,xx} = -f_{,yy} = \frac{+1}{4\pi(1-\nu)} \left[\frac{x-a}{(x-a)^2+y^2} - \frac{x+a}{(x+a)^2+y^2} \right]$$

$$f_{,xyy} = -f_{,xxx} = \frac{+1}{4\pi(1-\nu)} \left[\frac{(x-a)^2-y^2}{((x-a)^2+y^2)^2} - \frac{(x+a)^2-y^2}{((x+a)^2+y^2)^2} \right]$$

$$f_{,yyy} = -f_{,xxy} = \frac{+2y}{4\pi(1-\nu)} \left[\frac{x-a}{((x-a)^2+y^2)^2} - \frac{x+a}{((x+a)^2+y^2)^2} \right]$$